Cathodoluminescence Quantum Efficiency of Quantum Dot Thin Films

Heayoung P. Yoon[1,2*], Christopher D. Bohn[1], Youngmin Lee[1], , Seung-Hyeon Ko[1,2], Jonathan S. Steckel[3], Seth Coe-Sullivan[3], Nikolai B. Zhitenev[1]

[1] Center for Nanoscale Science and Technology, National Institute of Standards and Technology, Gaithersburg, MD 20899, United States

[2] Maryland Nanocenter, University of Maryland, College Park, MD 20742, United States

[3] QD Vision Inc., 29 Hartwell Ave., Lexington, MA 02421, United States

Abstract

A thin film of quantum dots (QD) was used to visualize the local photo-response of polycrystalline CdTe solar cells by down-converting an electron beam of high energy to photons of visible light. The efficient photon generation in the QD film is compared to cathodoluminescence of the high-purity bulk semiconductors and phosphor.

Keywords

quantum dot; thin film; cathodoluminescence; scanning electron microscopy.

1. Introduction

Traditional optical microscopy is a robust and universal scientific tool to acquire surface and sub-surface information from a sample. By scanning a laser beam, a laser beam induced current (LBIC) has been used to investigate lateral inhomogeneity in a variety of semiconductor devices and solar cells [1]. The excess carriers (*i.e.*, electron-hole pairs) in these methods are generated through local photon absorption. However, the resolution of far-field optical microscope is limited by diffraction (spatial resolution > $\lambda/2$; λ is wavelength). Advanced approaches of far-field optical microscopy have been demonstrated, yet the applications are limited to particular samples having either strong optical non-linearity or a sparse density of nanoscale features. Near-field scanning optical microscopy is a relatively slow technique and challenges remain in applications to samples having rough surfaces [2].

Recently, we reported a fast, high-resolution microscopy technique using cathodoluminescence (CL), where a conformal quantum dot film efficiently converts a high energy electron beam into a localized photon source addressable by an electron beam (Fig. 1) [3]. The Q-EBIC (EBIC using quantum dots) results were compared to the corresponding electron beam induced current (EBIC) data, showing distinct local carrier collection properties at grain interiors and grain boundaries at the wavelength of ≈ 620 nm in a polycrystalline cadmium telluride (CdTe) solar cell. The use of a bright local photon source is crucial to obtaining high quality Q-EBIC maps with this technique. However, the accurate determination of internal quantum efficiency of a thin film is challenging compared to bulk materials where thermopiles can be used [4]. In this paper, we assess the luminescence efficiency of quantum dot films by comparing CL characteristics with those of various semiconductors and phosphors at different electron beam voltages. Detailed analysis is presented using Monte Carlo simulation and finite-difference time domain calculations.

2. Experimental

A homogeneous film of cadmium selenide / zinc cadmium sulfide (CdSe / ZnCdS) core / shell quantum dots can be prepared by dip-coating, spin-coating, and drop-casting techniques. Figure 2 (a) shows a scanning electron microscopy (SEM) image of the uniform QD layers assembled on the planar substrate after the three dipping sequences [3]. The average diameter of the QDs is 9 nm ± 1 nm obtained using scanning transmission electron microscopy (STEM; Figure 2 b).

For the acceleration voltage dependent CL measurement, a thick layer of QD film (> 1 µm) was prepared by a drop-casting method onto a Si substrate (<0.005 Ω•cm) to reduce charging effects. Following the slow-dry of the QD solvent, another drop casting step was performed on top of the QD layer. Commercial quantum dots of QD1 (CdSe / CdS) and QD2 (CdSe / ZnS) were prepared using the same drop casting method. Spectroscopic ellipsometry was performed on the thick part of the QD film, where the CL spectra were collected. Commercial bulk wafers (≈ 400 µm thick) of GaAs, InP, and CdS were cleaned with acetone and isopropanol, and blown dry.

CL spectra were obtained using a Czerny-Turner spectrometer with a CCD (charged coupled device) camera, where the photons were collected by a diamond-tuned parabolic mirror and dispersed with a grating with a groove spacing of 150 mm^{-1}. The z-height (step size of 50 µm) was optimized by maximizing CL counts in the spectrum. The entrance slit to the spectrometer was wide open (1 mm) to maximize the collection of the CL photons, resulting in a broadening of the emission peaks but not affecting the integral count. The CL intensities of the CdSe / ZnCdS QD film, phosphor powder, and high-purity GaAs and InP were studied at different acceleration voltages. Figure 3 displays the measured CL spectra at 10 keV. The characteristic peak at each CL spectrum (with the exception of phosphor) is in agreement with the corresponding band-gap,

indicating band-edge recombination.

3. Results and Discussion

The internal quantum efficiency of CL of the CdSe / ZnCdS quantum dot film is compared to the bulk semiconductors, phosphor, and commercial quantum dots. The overall CL energy efficiency is given by

$$\eta = \frac{(1-r)[h\nu]}{\beta E_g} \cdot IQE_{CL} \cdot \eta_t \cdot \eta_{esc} \qquad \text{(Eq. 1)}$$

, where r is the backscattering coefficient, [$h\nu$] is the mean photon energy, βE_g is the energy needed to generate thermalized electron-hole pairs, η_t is the transfer efficiency of electron-hole pairs to emission centers, IQE_{CL} is the internal quantum efficiency, and η_{esc} is the probability of escape of the generated photons. Commercial phosphors and direct band-gap semiconductors would generally have high transfer efficiency ($\eta_t \approx 1$). η_{esc} is proportional to the CL fraction that was estimated using Equations 5 and 6.

Backscattered energy loss is associated with the primary electrons that leave the sample surface after one or several elastic or inelastic collisions. This loss depends on the atomic numbers or composition of the materials [5]. The remaining electron energy deposited in the sample is dissipated mostly through ionization events. Earlier experiments showed that the generation of one electron-hole pair corresponds to the loss of incident electron energy $\beta \times E_g$, where E_g is the energy band-gap of the material with $\beta \approx 3$ for many inorganic semiconductors and insulators [6]. The backscattered coefficient of each material was obtained from Monte Carlo simulations, shown in Figure 4. Table 1 summarizes the calculated maximum energy efficiency ($h\nu / \beta E_g$).

The fraction of cathodoluminescence depends on the refractive index of the materials, and

it has been modelled using both a simplified analytical approach as well as the rigorous solution of Maxwell's equations with a finite difference time domain technique. For the analytical model, light transmission (*T*) at an interface at normal incidence is determined from the Fresnel equations.

$$T \approx 1-\left(\frac{n_1-n_2}{n_1+n_2}\right)^2 \qquad \text{(Eq. 2)}$$

From Snell's law, light is transmitted from a medium 2 with a refractive index (n_2) to a medium 1 (n_1) when the illumination angle is below a critical value,

$$\phi_c = \sin^{-1}\left(\frac{n_1}{n_2}\right) \text{ and } n_2 > n_1 \qquad \text{(Eq. 3)}$$

Integrating the fractional area of a sphere (radius of *R*) gives:

$$\frac{\int_0^{2\pi}\int_0^{\phi_c} R^2 \sin(\phi)\, d\phi\, d\theta}{4\pi R^2} = \frac{\left[1-\cos(\phi_c)\right]}{2} = \frac{1}{2}\left[1-\sqrt{1-\left(\frac{n_1}{n_2}\right)^2}\right] \qquad \text{(Eq. 4)}$$

Thus, the total fraction of light transmitted from an incoherent, unpolarized point source incident on a planar interface can be approximated by combining the results from Equations 2 and 4 through multiplication

$$f_{CL} \approx \frac{1}{2}\left[1-\left(\frac{n_1-n_2}{n_1+n_2}\right)^2\right]\left[1-\sqrt{1-\left(\frac{n_1}{n_2}\right)^2}\right] \qquad \text{(Eq. 5)}$$

In the case of a stacked structure (Fig. 5b), where the top layer (n2) is relatively transparent (i.e., insignificant internal reflectance), the CL fraction from the medium 2 to medium 1 can be written as:

$$f_{CL2} \approx \frac{1}{2}\left[1-\left(\frac{n_1-n_2}{n_1+n_2}\right)^2\right]\left[1-\sqrt{1-\left(\frac{n_1}{n_2}\right)^2}\right] + \frac{1}{2}\left(\frac{n_2-n_3}{n_2+n_3}\right)^2\left[1-\left(\frac{n_1-n_2}{n_1+n_2}\right)^2\right]\left[1-\sqrt{1-\left(\frac{n_1}{n_2}\right)^2}\right] \qquad \text{(Eq. 6)}$$

, where the second term represents reflection off the bottom interface as shown in Fig. 5(b). However, the simplified analytical calculations do not take into account higher order interference effects which arise in thin films. While these numbers represent an approximation for a thick sample (thickness ≫ wavelength of CL), they will not be accurate for a thin film in a near-field regime. For such cases, we compute the CL fractions using a FDTD (Finite-Difference Time Domain) simulation, where a dipole source located at the center of the thin layer of interest represents the CL emission (Table 1).

Figure 6 compares the normalized CL signals accounting for the difference in the emission cone (CL fraction), the backscattered energy loss, and the number of generated CL photons (Table 1). Due to the refractive indices of the QD film (n = 1.9), InP (n = 3.3), and GaAs (n = 3.7) at the emission wavelengths (measured by spectroscopic ellipsometry), the fraction of the escaping photons from the materials to the vacuum is different. The CL fraction estimated from FDTD is 7 % for a QD film, 1.7 % for InP, and 1.2 % for GaAs. The estimated backscattered energy loss is ≈ 28 % for the QD film, ≈ 27 % for InP, and ≈ 22 % for GaAs from the Monte Carlo simulations. Optical losses may occur at the various optical components in the CL system (*e.g.*, grating, mirror, detector), and it was calibrated using commercial bulk materials. Assuming an IQE close to 100 % in the high purity GaAs or InP, we calculate the IQE of the QD film to be 102 % ± 7 %. This value is consistent with the IQE value determined in the Q-EBIC measurements in our previous publication, where the cathodoluminescence internal quantum efficiency is defined by the number of photons divided by the number of excited electron-hole pairs [3].

4. Conclusion

In summary, the quantum efficiency of cathodoluminescence of quantum dot film is determined from comparison with the bulk semiconductors, phosphor, and commercial quantum dots. The CL of the CdSe / ZnCdS quantum dot layer is bright with an internal quantum efficiency similar to that of high purity single crystalline semiconductors (*e.g.*, InP, GaAs).

5. Acknowledgements

H. P. Yoon, Y. Lee, and S. Ko acknowledge support under the Cooperative Research Agreement between the University of Maryland and the National Institute of Standards and Technology Center for Nanoscale Science and Technology, award 70NANB10H193, through the University of Maryland.

6. References

[1] (a) J. Marek, J Appl Phys 55 (2), 318-326 (1984). (b) J. Carstensen, G. Popkirov, J. Bahr and H. Foll, Sol Energ Mat Sol C 76 (4), 599-611 (2003).

[2] S. Smith, P. Zhang, T. Gessert and A. Mascarenhas, Appl Phys Lett 85 (17), 3854 (2004).

[3] H. P. Yoon, Y. Lee, C. D. Bohn, S. Ko, A. G. Gianfrancesco, J. S. Steckel, S. Coe-Sullivan, A. A. Talin and N. B. Zhitenev, AIP Advances 3, 062112 (2013).

[4] J. B. Birks, J Res Natl Stand Sec A 80 (3), 389 (1976).

[5] I. H. Campbell and B. K. Crone, Adv Mater 18 (1), 77-79 (2006).

[6] (a) C. A. Klein, IEEE J Quantum Elect QE-4 (4), 186-194 (1968). (b) B. Yacobi and D. Holt: Cathodoluminescence Microscopy of Inorganic Solids (Plenum, New York, 1990).

Figure 1. Schematic of Q-EBIC (EBIC using quantum dots). An irradiated electron beam on the quantum dots generates photons through cathodoluminescence. The emitted photons are absorbed in the CdTe, producing a local current.

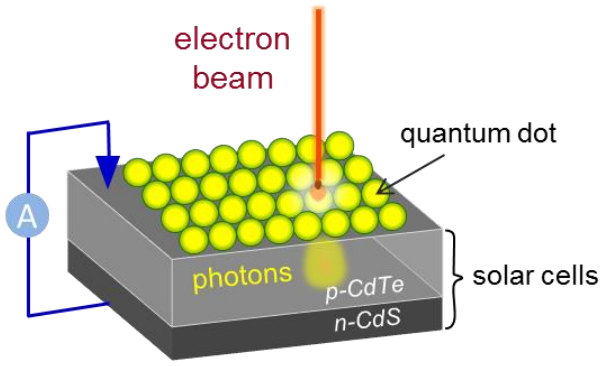

Figure 2. (a) An SEM image shows a highly-packed CdSe/ZnCdS QD laye. (b) A STEM image shows the diameter of the quantum dots to be 9 nm ± 1 nm.

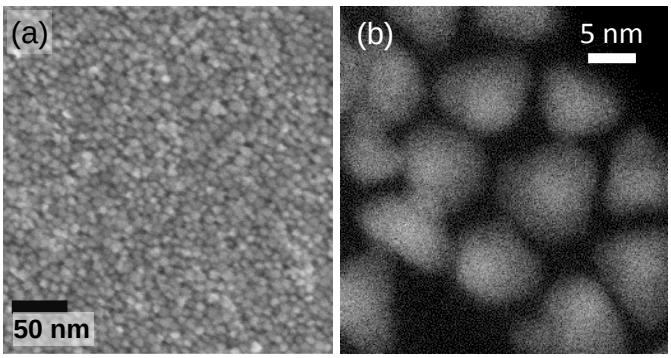

Figure 3. 10 keV CL spectra of various samples used in this work. The characteristic peaks correspond to the band-edge recombination (with the exception of phosphor).

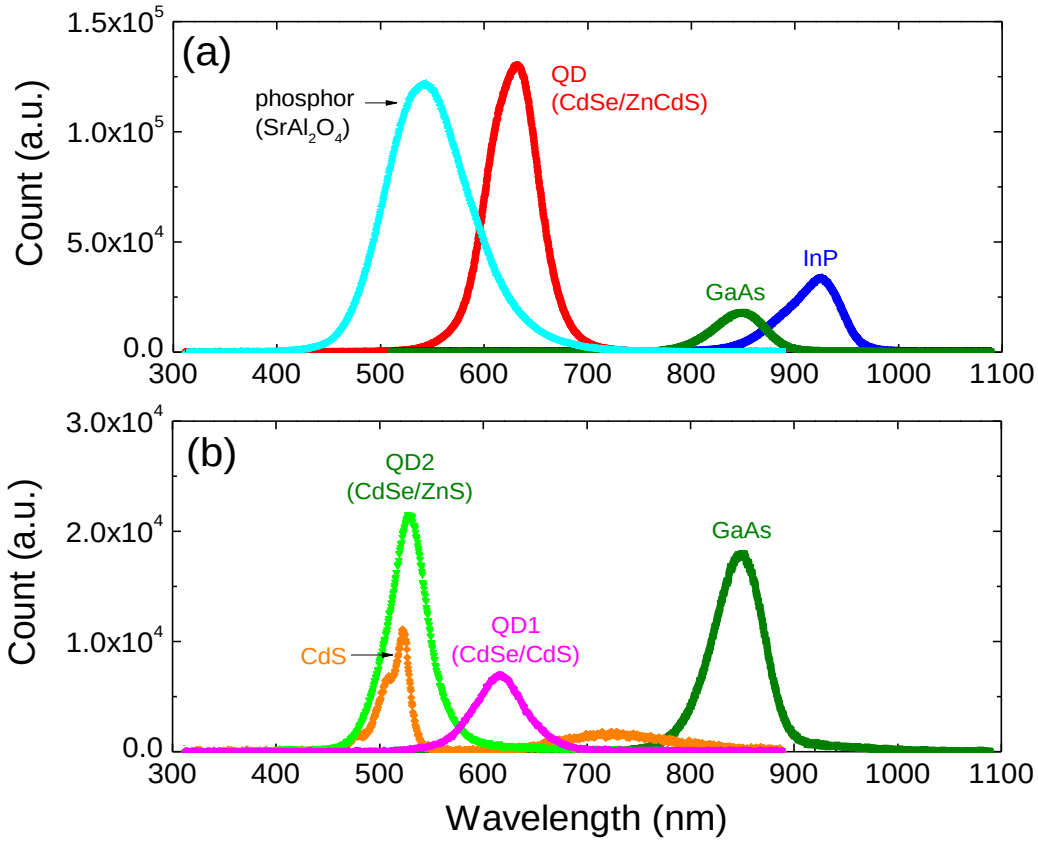

Figure 4. (a) Simulation of 3 keV electron beam irradiation of a bare CdTe layer. The energy of the secondary electrons is color coded from yellow (high energy) to blue (low energy). The backscattered electrons are shown in red. (b) Fraction of the backscattered electron energies at different acceleration voltages in each sample). The number of electrons simulated in the program could introduce one standard deviation uncertainty of E_{BSE} on the order of <5 %.

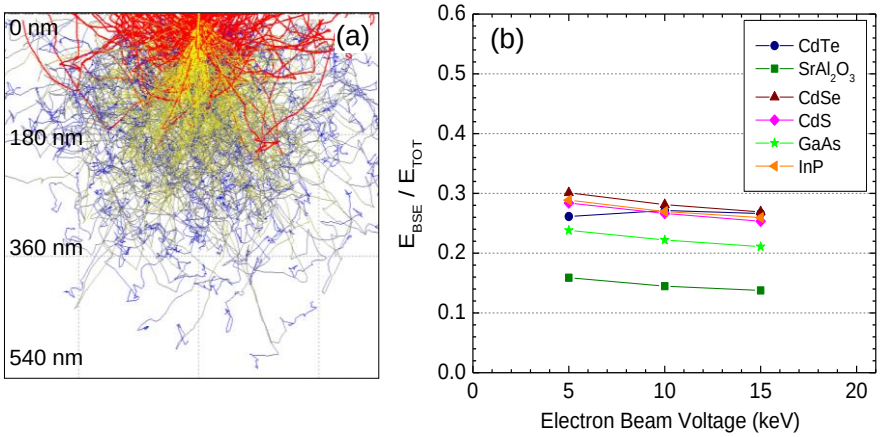

Figure 5. Fractional CL emission to vacuum from an incoherent, unpolarized dipole source in a bulk substrate (e.g., GaAs, InP; a) and stacked structure (e.g., QD film on a Si substrate; b).

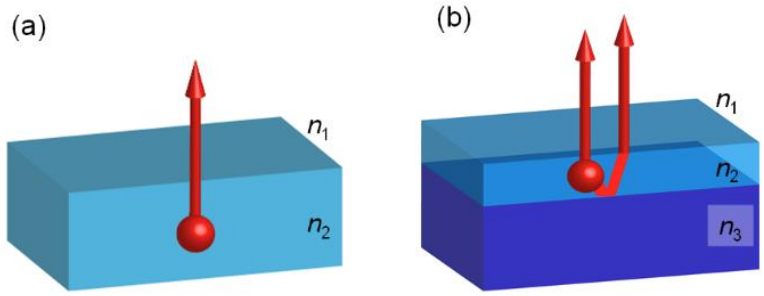

Figure 6. Total number of CL photons collected for 1s at different acceleration voltages. The electron beam current increases proportionally with acceleration voltage (239 pA at 5keV, 266 pA at 7 keV, 329 pA at 10 keV, 364 pA at 12 keV, and 422 pA at 15 keV). Representative error bars indicate one standard deviation uncertainties due to the spectroscopic collection setup and background signal of the CCD (charged coupled device) detector.

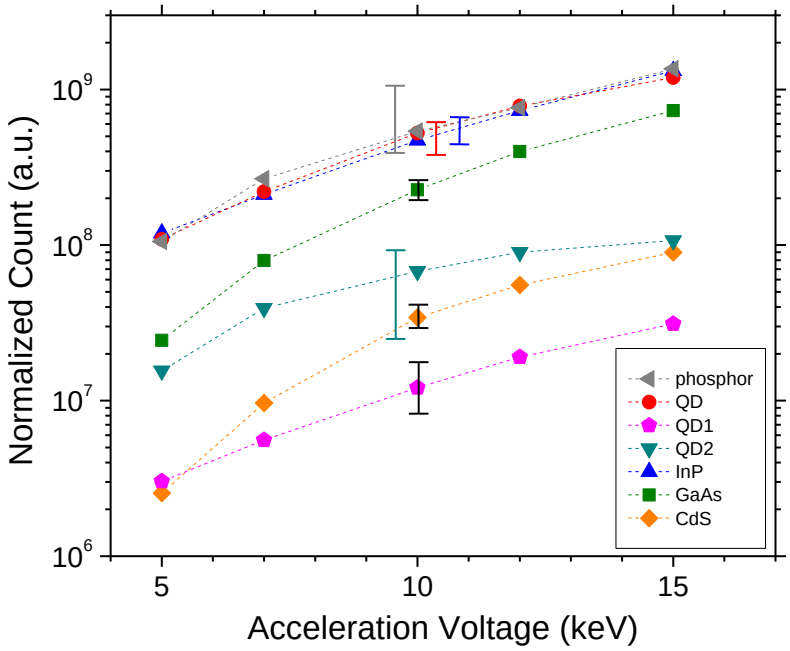

Table 1. Estimated maximum energy efficiency and fraction of CL emission [6].

*1. λ: peak wavelength extracted from the CL spectrum of each sample (technical specifications provided by vendors) .

*2. $\max \eta = \frac{[h\nu]}{\beta E_g} = \frac{hc}{3E_g\lambda}$: assumed that the backscatter coefficient (r) is 1 for all samples. [$h\nu$] is the mean photon energy, βE_g is the energy needed to generate thermalized electron-hole pairs h is Planck's constant, c is the speed of light in vacuum.

*3. n: Refractive index obtained from spectroscopic ellipsometery except QD1, QD2 (assumed the same value of CdSe/ZnCdS), and phosphor powder (one standard deviation uncertainty of n on the order of <5 % due to the spectroscopic collection setup).

*4. Estimated CL fraction (f_{CL}) using the Eq. (5) and Eq. (6). The probability of escape of the generated photons (η_{esc}) is proportional to the CL fraction.

*5. The backscattering coefficient (r) and the backscattered energy loss (BSE) of each material were calculated using Monte Carlo simulations.

*6. $\frac{\Sigma E_{CL}}{\text{e-beam energy}} \approx (1-r)(\max\eta)(\eta_t = 1)(\eta_{IQE})(f_{CL})$ · η_t is the transfer efficiency of electron-hole pairs to emission centers and η_{IQE} is the internal quantum efficiency.

	E_g (eV)	λ (nm)[*1]	Est. max. η (%)[*2]	n[*3]	Est. f_{CL} (%)[*4]	Est. r[*5]	Est. BSE (%)[*5]	Relative IQE (%)[*6]
QD1	2.0	635	33	1.9	7	0.38	28	7 ± 1
QD2	2.3	526	33	1.9	7	0.38	28	38 ± 7
CdS	2.4	516	33	2.4	3.8	0.37	27	16 ± 1
GaAs	1.45	850	33	3.7	1.2	0.32	22	98 ± 4
InP	1.35	920	33	3.3	1.7	0.37	27	100 ± 6
Phosphor	6.5	520	12	1.7	8.9	0.22	15	N/A
CdSe/ZnCdS	2	620	33	1.9	7	0.38	28	102 ± 7